Nonlinear Processes in Geophysics (1998) 5: 81–92

Nonlinear Processes in Geophysics

On the nonlinear dynamics of rupture

H. Ockendon[1] and D. L. Turcotte[1,2]

[1]Center for Industrial and Applied Mathematics, Mathematical Institute, Oxford OX1 3CB, England
[2]Department of Geological Sciences, Cornell University, Ithaca, NY 14853, USA

Received: 19 December 1996 – Accepted: 21 July 1998

Abstract. The rupture on a fault resulting in an earthquake is clearly a complex process. In order to better understand this process the continuum version of the slider-block model has been considered in some detail. In particular, the role of a cohesive breakaway zone is considered. Solutions of a "piston" problem and a "shock-tube" problem are obtained. For the "driven" problem the cohesive breakaway solution is combined with a viscous resistance on the fault to obtain solutions that are reasonably realistic in terms of fault rupture.

1 Introduction

Earthquakes are generally associated with ruptures on preexisting faults. One of the remarkable features is that there are no reliable precursors to warn that an earthquake is about to occur; for example, there is no consistent precursory seismic activity or strain. In order to better understand earthquakes, it is essential to develop a better understanding of how earthquakes nucleate and how rupture proceeds

Although it is generally accepted that earthquakes are associated with displacements on preexisting faults, it must be recognized that both the fault and the media in which it is embedded are extremely complex. The fault itself is a zone of granulated material (fault gouge) that is neither planar nor uniform is physical properties. The surrounding media is also extensively fractured and contains other faults on all scales.

Despite the recognized complications, it is clearly desirable to study relatively simple rupture models in order to better understand earthquakes. As a first approximation, it is acceptable to assume that the friction between fault surfaces dominates the physics of rupture initiation and propagation. Extensive laboratory studies have been carried out to determine the frictional behavior of rock surfaces and fault gouge but the applicability of the results to actual faults has been questioned (Scholz, 1990, pp. 91-96).

It is recognized that velocity weakening is a necessary condition for stick-slip behavior, rather than stable sliding on a fault. Amonton's law is generally applied to faults so that the shear stress τ on a fault is given by

$$\tau = f\,(\rho g h - p_h) \tag{1}$$

where f is the coefficient of friction, $\rho g h$ the lithostatic pressure, and p_h the fluid pressure. The simplest approach to friction is the static-dynamic model. If the slip velocity is zero, $v = 0$, the static coefficient of friction f_s is applicable; if the slip velocity is non zero, $v>0$, the dynamic coefficient of friction f_d is applicable. As long as $f_s > f_d$, stick-slip behavior is expected. But this model is clearly an oversimplification, the next degree of complexity is to have a functional dependence of friction on slip velocity, an example is

$$f = \frac{f_s}{\left(1 + \frac{v}{v_c}\right)^n} \tag{2}$$

where v_c is a characteristic velocity. However, laboratory experiments have shown that friction does not immediately adjust to a new slip velocity. This led to the introduction of one or more state variables (Dieterich, 1978, 1979; Ruina, 1983; Blanpied and Tullis, 1986; Kosloff and Liu, 1980; Linker and Dieterich, 1992; Weeks, 1993; Okubo and Dieterich, 1986). A typical example with a single state variable is (Okubo, 1989)

$$f = f_o + b \log (b_1\,\vartheta + 1) - a \log\left(\frac{a_1}{v} + 1\right) \tag{3}$$

$$\frac{d\vartheta}{dt} = 1 - \frac{\vartheta v}{D_c} \tag{4}$$

where ϑ is the state variable and f_o, b, b_1, a, a_1, and D_c are empirical constants

The state variable is generally associated with the time dependence of surface adhesion (Dietrich, 1972; Pollock, 1992). Dieterich and Conrad (1984) describe the physics as follows: "A change in slip velocity produces an immediate change in frictional resistance that is of the same sign as the change in velocity. However, as slip progresses at the new

Correspondence to: H. Ockendon

velocity, the age of the load bearing contacts begins to evolve to a new population with an average age that is characteristic of the new velocity".

The essential question that must be addressed is whether the empirical friction laws based on laboratory studies are applicable to actual faults. Of necessity, the laboratory experiments must be carried out at much lower velocities (typically 10^{-6} m/s) than slip velocities on real faults (up to 1 m/s). However, it has also been questioned whether the results are applicable in terms of static friction. Based on their own experimental results, Beeler et al. (1994) argue that the presently accepted friction laws are inadequate to predict real fault behavior. They suggest a much stronger time dependence with a "healing" of a ruptured fault to prevent a subsequent slip.

One immediate objection to the rate and state friction law given in (3) and (4) is that the friction coefficient is infinite when $v = 0$, i.e. the static coefficient of friction is infinite. This has led some authors to suggest that faults are always slipping at very low velocities, a very doubtful suggestion. However, modifications of the friction law can be made relatively easily to overcome this objection.

A much more serious objection to the applications of the laboratory derived frictions laws to actual faults is the predicted high stress levels and low stress drops. Earthquakes often nucleate at a depth of 10 km where the lithostatic pressure is 250 Mpa, a typical static failure stress would be 10 Mpa, giving a coefficient to static friction $f = 0.04$ while typical laboratory values are $f = 0.6$. Recognizing this major discrepancy a number of authors have proposed that the low stress is due to a high fluid pressure (Byerlee, 1990; Blanpied et al., 1992; Sleep and Blanpied, 1992, 1994). This requires an impermeable fault zone and several mechanisms have been proposed; but at best, this proposal must be considered ad hoc. The stress paradox strongly reinforces other objections to currently accepted concepts of friction on faults.

The rate and state equations predict measurable slip on faults in the interseismic period between major earthquakes. Since the lithostatic normal force increases linearly with depth, it is also expected that the frictional resistance to slip also increases with depth. As the stress on a fault increases during as earthquake cycle it would be expected that slip would occur on the upper portion of the fault while it remains locked at depth (Tse and Rice, 1986; Lorenzetti and Tullis, 1989; Rice, 1993). While there are exceptions, observations, either directly or geodedically, of such fault offsets are quite rare. The locked northern and southern sections of the San Andreas fault are not slipping. On the basis of high resolution strain and tilt data Johnston et al. (1987) found no precursory fault displacements prior to several earthquakes in California. These authors suggest: "that rupture initiation occurs at smaller regions of higher strength which, when broken, allow runaway catastrophic failure".

Many authors have recognized that classic laboratory frictional behavior may not be applicable to real faults and a variety of alternative hypotheses for rupture mechanics have been proposed. It has been proposed that the granular fault gouge becomes acoustically fluidized during rupture (Melosh, 1979, 1995). Under rather restricted conditions sufficient energy is available to fluidize a narrow zone of fault gouge. Heaton (1990) pointed out that self healing "Heaton" pulses are inconsistent with classic friction experiments and suggested that fault gouge may become acoustically fluidized when a critical slip velocity is exceeded. Fluidization could certainly reduce the dynamic friction on a fault but would not be expected to reduce the static friction.

A second approach to dynamic rupture on faults invokes interface waves. Brune et al. (1993) and Anooshelpoor and Brune (1994) have proposed interface waves involving fault surface separation during slip (Schallamach, 1971, Mora and Place, 1994). They also suggest that normal interface vibrations associated with these waves can explain the high corner frequency. A number of authors have considered the role of normal vibrations on friction (Tolstoi, 1967; Comninou and Dundurs, 1977, 1978; Freund, 1978) and several have concluded that the excitation of Rayleigh waves on a rupture surface can lead to periodic pulses of separation; however, this mechanism is controversial and has not been demonstrated experimentally in a conclusive manner.

Several authors have recently included a linear viscous resistance on the slip surface (Nakanishi, 1994; Morgan et al., 1997). A Barenblatt cohesive zone is introduced at the crack tip and this cohesion models the static friction. With a viscous resistance to slip on the crack surface, the tip singularity is reduced below the value 1/2 associated with the classic stress intensity factor and the velocity of crack propagation is a function of the crack "viscosity". Rupture always initiates at the same value of the cohesive force independent of the viscosity and the rupture velocity increases towards the relevant sound speed as the viscosity is decreased. These authors suggest that there are two slip-mode regimes during earthquake rupture. In the immediate vicinity of the crack tip, slip velocities are small and cohesive forces dominate. This is the regime that has been studied in the laboratory; plastic deformation of the surfaces and gouge dominate and the "frictional" stress is relatively high. At higher slip velocities, away from the crack tip, there is a second frictional mode with low frictional stresses. This second mode may be due to acoustic fluidization or separation waves. A linear viscous rheology is consistent with the fluidization of fault gouge (Savage, 1984; Campbell, 1990). As the driving stress drops, the slip velocity decreases, there is a return to the cohesive mode, and the fault heals.

Solutions of the full equations of elasticity for a propagating fracture are obscured by the mathematical difficulties associated with the crack tip. A model that retains the physics while considerably reducing the mathematical difficulty was introduced by Burridge and Knopoff (1967). They considered a series of slider blocks which were pulled over a surface by driver springs and connected to each other by connector springs. The simplest model is to consider a pair of interacting slider blocks. It has been shown that this system can exhibit chaotic behavior (Huang and Turcotte, 1990, 1992; Narkounskaia and Turcotte, 1992).

This model was extended to long linear arrays of slider blocks by Carlson and Langer (1989) and Carlson et al. (1991). They used a velocity-weakening friction law and considered up to 400 blocks. Slip events involving large numbers of blocks were observed, the motion of all blocks

involved in a slip event were coupled and the applicable equations of motion had to be solved simultaneously. Although the system is completely deterministic, the behavior was apparently chaotic. Frequency-size statistics were obtained for slip events and the events fell into two groups, smaller events obeyed a power-law (fractal) relationship but there were an anomalously large number of large events that included all the slider blocks.

Nakanishi (1990, 1991) proposed a model that combined features of the cellular-automata model and the slider-block model. A linear array of slider-blocks was considered but only one block was allowed to slide at a time. Thus interactions were only with nearest neighbors, which would then be allowed to slip in a subsequent step, until all blocks were again stable. Brown et al. (1991) proposed a modification of this model involving a two-dimensional array of blocks. Other models of this type have been considered by Takayasu and Matsuzaki (1988), Ito and Matsuzaki (1990), Sornette and Sornette (1989, 1990), Langer and Tang (1991), Carlson (1991a, b), Carson et al. (1993a, b), Matsuzaki and Takayasu (1991), Rundle and Brown (1991), Shaw et al. (1992), Huang et al., (1992), Feder and Feder (1991), Vasconcelos et al. (1992), Christensen and Olami (1992), Knopoff et al. (1993), Rundle and Klein (1993), Pepke and Carlson (1994), Pepke et al. (1994). The behavior of linear arrays of slider blocks without a puller plate has been considered by de Sousa Vieira (1992), de Sousa Vieira et al. (1993) and by de Sousa Vieira and Herrmann (1994).

If the connector springs are stiff compared to the driver springs a continuum approximation can be written (Langer and Tang, 1991) and the governing equation becomes the telegraph equation. A variety of studies in this limit have been carried out (Langer 1992, 1993; Langer and Nakanishi 1993; Myers and Langer 1993). A series of studies in this limit will be carried out in this paper.

2 The model

Consider the infinite array of slider blocks illustrated in Fig. 1. Each block has a mass m and is connected to a driver plate by a spring with spring constant k_p; adjacent blocks are connected by springs with spring constant k_c. The displacement of the driver plate is w_p and the displacement of the nth block in the +x-direction is w_n. The motion of the nth block is resisted by the frictional force F_n. The equation of motion of the nth block is

$$m\frac{\partial^2 w_n}{\partial t^2} + k_c\,(w_n - w_{n-1} + w_n - w_{n+1}) - k_p\,(w_p - w_n) = F_n \qquad (5)$$

For stiff connector springs, k_c large, the variation of w_n with n will be small so that it is appropriate to make the approximation

$$w_{n+1} - w_n - w_n + w_{n-1} = \delta^2\frac{\partial^2 w}{\partial x^2} \qquad (6)$$

where δ is the separation between blocks. We further assume that the stiffness is sufficiently high that we can assume that variations in δ are small, we assume δ is a constant. A wave

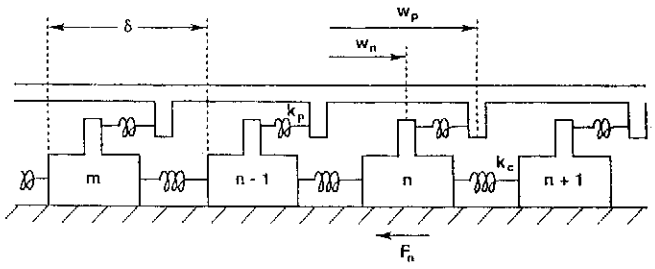

Fig. 1. Illustration of an infinite linear array of slider blocks. Each block has a mass m, and is attached to a driver plate with a spring (spring constant k_p). Adjacent blocks are separated by a distance δ and are connected to each other by springs (spring constant k_c). The blocks are listed sequentially ..., n - 1, n, n +1, ... and the frictional force resisting the forward motion of block n is F_n. The position of the driver plate is w_p (t) and the position of block n is w_n.

speed can be defined by

$$c = \left(\frac{\delta^2 k_c}{m}\right)^{1/2} \qquad (7)$$

so that in this limit (5) becomes

$$m\frac{\partial^2 w}{\partial t^2} - m\,c^2\frac{\partial^2 w}{\partial x^2} - k_p\,(w_p - w) = -F \qquad (8)$$

In terms of a model for a fault, the first term represents inertia, the second term elasticity, the third term the driving stress, and the right side the frictional resistance and/or cohesion.

In order to relate the simple slider-block model to the behavior of a real fault we introduce the density ρ and elastic modulus μ of the material and write

$$c = \rho\,A\,\delta \qquad (9)$$

$$\mu = \frac{\delta k_c}{A} \qquad (10)$$

where A is the area of a block. Combining (7), (9), and (10) gives

$$c = \left(\frac{\mu}{\rho}\right)^{1/2} \qquad (11)$$

which is a standard result for a one-dimensional sound speed. Typical values for rock are μ = 30 Gpa and ρ = 3,000 kg/m^3 which gives c = 3km/s.

Our governing equation has been given in (8). We will now consider a number of solutions in order to better understand the basic physics of the rupture propagation problem as modeled by (8). We will consider three effects:

1) The role of cohesion at the crack tip. The cohesion will be shown to be equivalent to the Griffith energy criteria for the onset of fracture. It is also one way to represent the transition from static to dynamic friction.

2) The role of a viscous resistance on the rupture surface. We will consider a frictional resistance that increase linearly with the slip velocity. The linear assumption is a mathematical convenience to maintain the linearity of the equations, but we will conclude that a frictional resistance that increases with

velocity is a necessary feature of any model for the propagation of earthquake ruptures.

3) The role of the driver springs in models of rupture propagation. Without driver springs realistic solutions can be obtained without a viscous resistance, with driver springs a viscous resistance is essential.

3 Piston driven motion with cohesion

As our first specific example we will assume that the linear array of blocks are driven to the right by a piston as illustrated in Fig. 2. The blocks are connected to each other but not to a driver plate so that the governing equation (8) becomes

$$m\frac{\partial^2 w}{\partial t^2} - mc^2\frac{\partial^2 w}{\partial x^2} = -F \qquad (12)$$

The piston moves at a constant velocity u_p so that its position is $w_o = u_p t$. If the frictional force F is zero a breakaway wave moves to the right at the speed of sound c and the velocity of the blocks behind the breakaway wave is u_p, i.e.

$$\begin{aligned} w &= 0 && \text{if } x > ct \\ w &= u_p\,(t - x/c) && \text{if } w_0 < x < ct \end{aligned} \qquad (13)$$

The force F_p on the piston is given by

$$F_p = -\delta k_c\frac{\partial w}{\partial x} = \delta k_c\frac{u_p}{c} = (mk_c)^{1/2}u_p \qquad (14)$$

And the work done per unit time by the piston, power input P_i, is given by

$$P_i = F_p u_p = (mk_c)^{1/2}u_p^2 \qquad (15)$$

The number of blocks that breakaway per unit time is c/δ so that the kinetic energy imparted to the blocks per unit time P_{KE} is

$$P_{KE} = \frac{1}{2}mu_p^2\frac{c}{\delta} = \frac{1}{2}(mk_c)^{1/2}u_p^2 \qquad (16)$$

And the potential energy per unit time imparted to the springs P_{PE} is

$$P_{PE} = \frac{1}{2}k_c\delta^2\left(\frac{\partial w}{\partial x}\right)^2\frac{c}{\delta} = \frac{1}{2}(mk_c)^{1/2}u_p^2 \qquad (17)$$

And as expected we have

$$P_i = P_{KE} + P_{PE} \qquad (18)$$

Half the energy input from the piston goes into kinetic energy of the masses and half into the potential energy of the connector springs.

We assume that the driving stress σ is given by

$$\sigma = \frac{F_p}{A} \qquad (19)$$

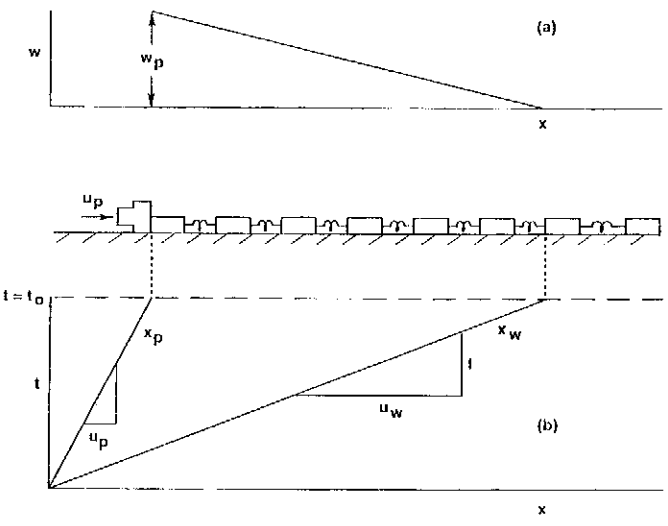

Fig. 2. Illustration of a semi-infinite, linear array of slider blocks driven to the right by a piston moving at a constant velocity u_p. The breakaway wave propagates to the right with a speed u_w. In (a) the position of the blocks w is given as a function of position x at $t = t_o$. In (b) the positions of the piston x_p and breakaway wave x_w are given as a function of time.

Substitution of (9), (10), and (14) into (19) gives

$$\sigma = (\rho\,\mu)^{1/2}u_p \qquad (20)$$

A typical velocity for an earthquake is $u_p = 1$ m/s. Taking this value along with those given above we have $\sigma = 10$ Mpa, a very typical value for shear stress prior to an earthquake. Thus a simple force balance without either static or dynamic friction produces values typically observed in real earthquakes.

On faults, breakaway is resisted by the cohesion of the fault surfaces. We will apply the Barenblatt (1968) criteria and assume that the force resisting breakaway is a constant g_o until a breakaway displacement is reached. That is

$$\begin{aligned} F &= g_o && \text{for } 0 < w < w_b \\ F &= 0 && \text{for } w > w_b \end{aligned} \qquad (21)$$

The ultimate propagating breakaway wave will now have structure and propagate at a constant speed u_b which is less than the sound speed, $u_b < c$. In order to determine this structure we transform to a wave-fixed coordinate system using

$$\xi = x - u_b t \qquad (22)$$

In terms of the new variable ξ and (21), (12) becomes

$$\begin{aligned} (c^2 - u_b^2)\frac{d^2w}{d\xi^2} &= \frac{g_o}{m} && \text{for } \xi > 0 \\ (c^2 - u_b^2)\frac{d^2w}{d\xi^2} &= 0 && \text{for } \xi > 0 \end{aligned} \qquad (23)$$

We assume breakaway occurs at $\xi = 0$ so that $w = w_b$ at $\xi = 0$.

In the upstream region $\xi > 0$ the solution of (23) is

$$w = \frac{1}{(c^2 - u_b^2)}\left[\frac{g_o\xi^2}{2m} + C_1\xi + C_2\right] \qquad (24)$$

We satisfy the boundary conditions $w = dw/d\xi = 0$ at $\xi = \xi_o$, where ξ_o is the front of the traveling wave and $w = w_b$ at $\xi = 0$ and obtain

$$w = \frac{1}{(c^2 - u_b^2)\, m}\left(\frac{1}{2}\xi^2 - \xi\xi_o\right) + w_b \quad \text{for } 0 < \xi < \xi_0 \tag{25}$$

where

$$\xi_o = \left[\frac{2m\, w_b}{g_o}\left(c^2 - u_b^2\right)\right]^{1/2} \tag{26}$$

In the downstream regions $\xi < 0$ we require as the solution of (23)

$$w = C'_1 + C'_2\, \xi \tag{27}$$

And as boundary conditions we require $w = w_b$ at $\xi = 0$ and in order to have the constant piston velocity u_p we have

$$\frac{dw}{d\xi} = -\frac{1}{u_b}\frac{\partial w}{\partial t} = -\frac{u_p}{u_b} \tag{28}$$

With these conditions (27) becomes

$$w = w_b - \frac{u_p}{u_b}\xi \quad \xi<0 \tag{29}$$

In addition we require the continuity of $dw/d\xi$ at $\xi = 0$ so that

$$\frac{u_p}{u_b} = \left[\frac{2\, g_o\, w_b}{m\left(c^2 - u_b^2\right)}\right]^{1/2} \tag{30}$$

And this can be solved for the wave speed u_b with the result

$$\frac{u_b}{c} = \frac{1}{\left(1 + \dfrac{2g_0\, w_b}{m\, u_p^2}\right)^{1/2}} \tag{31}$$

The nondimensional quantity $2\, g_0\, w_b/mu_p^2$ is the ratio of the work required to overcome cohesion $g_o\, w_b$ to the kinetic energy of a moving block $mu_p^2/2$. The larger the cohesive work, the more the propagation velocity is reduced below the sound speed c. The solution in the vicinity of the breakaway point is given in Fig. 3.

The force F_p on the piston is now given by

$$F_p = \delta\, k_c\, \frac{u_p}{u_b} = \left(m\, k_c\right)^{1/2} u_p \left(1 + \frac{2g_o\, w_b}{m\, u_p^2}\right)^{1/2} \tag{32}$$

which reduces to (14) when the cohesive force is negligible. The power input is

$$P_i = \left(m\, k_c\right)^{1/2} u_p^2 \left(1 + \frac{2g_o w_b}{m\, u_p^2}\right)^{1/2} \tag{33}$$

The number of blocks that breakaway per unit time is u_b/δ so that the power that goes into kinetic energy is

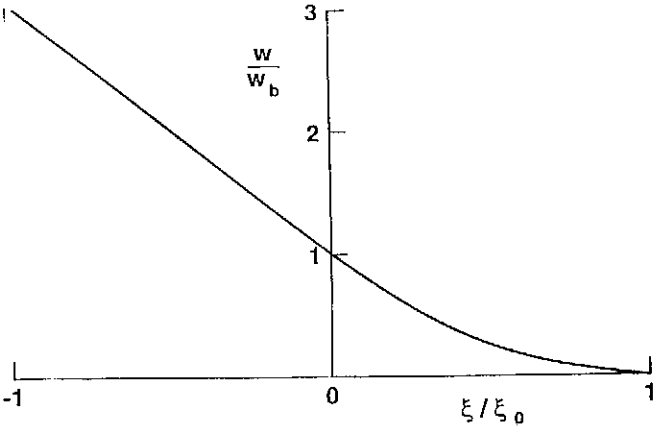

Fig. 3. Upstream solution in the cohesion zone, $0 < \xi/\xi_0 < 1$, from (25) matched to downstream solution from (29). Breakaway takes place at $\xi = 0$.

$$P_{KE} = \frac{1}{2}\, m\, \frac{u_p^2\, u_b}{\delta} = \frac{\frac{1}{2}\left(m\, k_c\right)^{1/2} u_p^2}{\left(1 + \dfrac{2\, g_o\, w_b}{m\, u_p^2}\right)^{1/2}} \tag{34}$$

The potential energy imparted to the springs is

$$P_{PE} = \frac{1}{2}\, k_c\, \delta^2 \left(\frac{\partial w}{\partial x}\right)^2 \frac{u_b}{\delta} = \frac{1}{2}\left(m\, k_c\right)^2 u_p^2 \left(1 + \frac{2\, g_o\, w_b}{m\, u_p^2}\right)^{1/2} \tag{35}$$

And the energy per unit time required to break cohesion is

$$P_c = g_o\, w_b\, \frac{u_b}{\delta} = \frac{g_o\, w_b \left(k_c/m\right)^{1/2}}{\left(1 + \dfrac{2g_o\, w_b}{m\, u_p^2}\right)} \tag{36}$$

As expected we have

$$P_i = P_{KE} + P_{PE} + P_c \tag{37}$$

It is also interesting to note that

$$P_{PE} = P_{KE} + P_c \tag{38}$$

The potential energy in the springs is equal to the sum of the kinetic energy of the blocks and the energy required to overcome cohesion.

It is convenient to relate the cohesive force g_o to a cohesive stress σ_c with

$$g_o = \sigma_c\, \delta \sqrt{A} \tag{39}$$

Introducing (39) into the definition of the nondimensinal cohesion parameter C we obtain

$$C = \frac{2g_0\, w_b}{m\, u_p^2} = \frac{2\, \sigma_c\, w_b}{\rho \sqrt{A}\, u_p^2} \tag{40}$$

Taking the cohesion parameter equal to unity we obtain

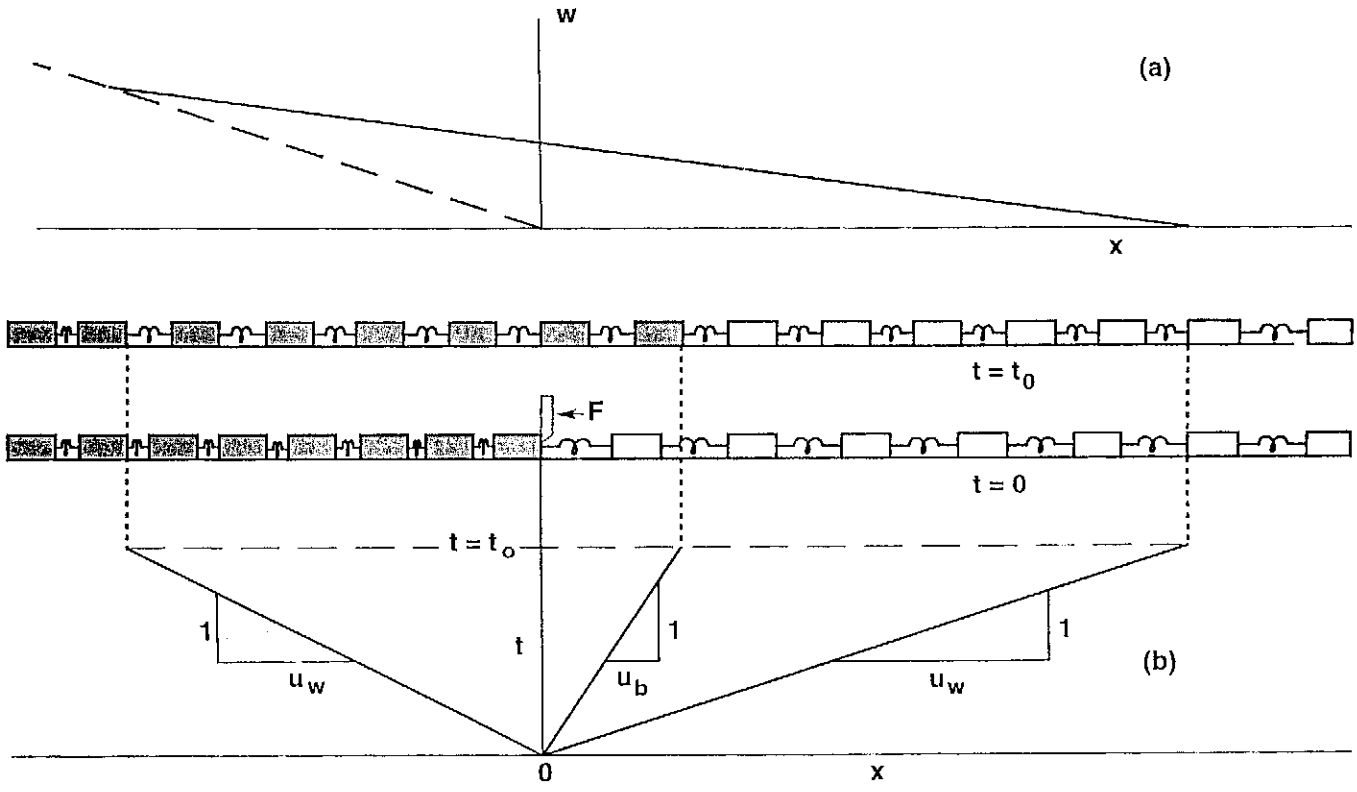

Fig. 4 Illustration of the "shock-tube" problem in an infinite linear array of slider blocks. For $t < 0$ all blocks are stationary, springs in $x > 0$ are uncompressed, and springs in $x < 0$ are compressed so that they have a uniform compressional force F_o. At $t = 0$ the restraint at $x = 0$ is removed and breakaway waves move upstream and downstream at the sound speed c. Between the breakaway waves all blocks are moving to the right with a speed u_o. In (a) the positions of the blocks w (x) are given at $t = 0$ (dashed line) and at $t = t_o$ (solid line). In (b) the positions of the breakaway waves x_w and the movement of the block initially at $x = 0$, x_p, are given.

$$\sigma_c \; w_b = \frac{1}{2} \rho \, u_p^2 \sqrt{A} \qquad (41)$$

Taking $\rho = 3{,}000$ kg/m^3, $u_p = 1$ m/s, and $\sqrt{A} = 1$ km we find that $\sigma_c \, w_b = 1.5 \times 10^6$ Pa m. If $\sigma_c = 30$ M Pa we require $w_b = 0.05$ m, probably reasonable values.

4 "Shock tube" problem

In order to further illustrate the behavior of breakaway waves we consider a "shock tube" problem. In a shock tube, a high pressure gas is separated from a low pressure gas by a diaphragm. When the diaphragm is broken a compression wave propagates upstream into the low pressure section and an expansion wave propagates downstream into the high pressure section. If the pressure difference is small, both waves propagate at the speed of sound in the gas.

We consider an infinite linear array of slider blocks connected by springs. Initially, at $t = 0$, all springs in $x > 0$ are uncompressed ($F_p = 0$) and all springs in $x < 0$ are compressed by a force F_o, i.e.

$$\begin{aligned} w &= 0 && \text{at } t = 0,\ x < 0 \\ w &= -\frac{F_0}{\delta k_c} \; x && \text{at } t = 0,\ x < 0 \end{aligned} \qquad (42)$$

There is a discontinuity in the spring force at $x = 0$ for $t < 0$, at $t = 0$ this forced discontinuity is removed, this is equivalent to the breaking of the diaphragm in the shock tube.

Once again (12) is applicable. If the frictional force is zero, breakaway waves are expected to propagate both upstream (compressional) and downstream (expansion) at the speed of sound c as illustrated in Figure 4. All blocks between the two waves are expected to move to the right with a constant velocity u_o, i.e.

$$\begin{aligned} u &= 0 && x > ct \\ u &= u_o && -ct < x < ct \\ u &= 0 && x < -ct \end{aligned} \qquad (43)$$

The force compressing the blocks behind the compressional wave F_u is given by (14) and can be written

$$F_u = (m \, k_c)^{1/2} \, u_u \qquad (44)$$

And the force compressing the blocks behind the expansion wave F_{bd} is given by

$$F_o - F_d = (m \, k_c)^{1/2} \, u_d \qquad (45)$$

However we require $u_u = u_d = u_o$ and $F_d = F_u = F_b$ and from (44) and (45) find that

$$F_b = \frac{1}{2} F_o \tag{46}$$

$$u_o = \frac{F_o}{2 (m k_c)^{1/2}} \tag{47}$$

The springs in the breakaway region have one-half the force F_o in the driving region. In direct analogy with (13) the solution to this problem is

$$\begin{aligned} w &= 0, && x > ct \\ w &= \frac{F_o}{2 \delta k_c} (ct - x) && -ct < x < ct \\ w &= -\frac{F_o x}{\delta k_c} && x < -ct \end{aligned} \tag{48}$$

This solution is illustrated in Fig. 4.

Again we carry out an energy balance. The input energy comes from the potential energy of the downstream springs that enter the breakaway zone and is given by

$$P_i = \frac{1}{2} \frac{F_o^2}{k_c} \frac{c}{\delta} = \frac{1}{2} \frac{F_o^2}{(k_c m)^{1/2}} \tag{49}$$

The kinetic energy imparted to the blocks in the breakaway wave per unit time is

$$P_{KE} = \frac{1}{2} m u_b^2 \, 2 \frac{c}{\delta} = \frac{1}{4} \frac{F_o^2}{(k_c m)^{1/2}} \tag{50}$$

And the potential energy imparted to the springs in the breakaway region per unit time is

$$P_{PE} = \frac{1}{8} \frac{F_o^2}{k_c} \, 2 \frac{c}{\delta} = \frac{1}{4} \frac{F_o^2}{(k_c m)^{1/2}} \tag{51}$$

Again the energy balance (18) is satisfied and half the energy input goes into kinetic energy and half into potential energy.

We will next expand the shock tube problem to include cohesion forces in both upstream and downstream breakaway waves. We again assume the Barenblatt (1962) condition (21) and the solution given above for the piston problem is directly applicable to the upstream breakaway wave and it can be easily modified to provide the structure of the downstream breakaway wave. The upstream breakaway compression wave propagates to the right with a velocity u_b, the downstream beakaway expansion wave propagates to the left with a velocity $-u_b$. The force in the breakaway region F_b is one half the driving force F_o, $F_b = F_o/2$, as was the case without cohesion.

The entire solution can be written

$$w = 0, \qquad x > u_b t + \xi_o \tag{52}$$

$$w = \frac{g_o}{m (c^2 - u_b^2)} \left[\frac{1}{2} (x - u_b t)^2 - (x - u_b t) \xi_o \right] + w_b, \qquad u_b t < x < u_b t + \xi_o \tag{53}$$

$$w = -\frac{F_o}{2 \delta k_c} (x - u_b t) + w_b, \qquad -u_b t < x < u_b t \tag{54}$$

$$w = -\frac{F_o x}{\delta k_c} + \frac{g_o}{m (c^2 - u_b^2)} \left[\frac{1}{2} (x + u_b t)^2 + (x + u_b t) \xi_o \right] + w_b, \quad -u_b t, \; -\xi_o < x < -u_b t \tag{55}$$

$$w = -\frac{F_o x}{\delta k_c} \qquad x < -u_b t - \xi_o \tag{56}$$

where the thickness of the cohesive zones is again given by (26). The continuity of $\partial w/\partial x$ at $x = \pm u_b t$ again gives the wave speed with the result

$$u_b = c \left(1 - \frac{8 k_c w_b g_o}{F_o^2} \right)^{1/2} \tag{57}$$

The nondimensional parameter $2 k_c w_o g_o/F_0^2$ is the ratio of the work required to overcome cohesion of a block $w_b g_o$ to the potential energy initially stored in a downstream spring $F_0 /2 k_c$. In order for a breakaway wave to propagate in the shock tube configuration the stored energy per spring must be greater than four times the cohesive energy per block.

It is again of interest to examine the analogy to a real fault. Introducing (10), (19), and (39), the propagation condition becomes

$$\sigma_o = \left(\frac{8 w_b \sigma_c \mu}{\sqrt{A}} \right)^{1/2} \tag{58}$$

This relation is closely related to the standard theory for stress-intensity factors. The definition of the stress intensity factor in terms of the stress σ, a distance r from a crack tip is

$$\sigma_r = \frac{K}{\sqrt{2 \pi r}} \tag{59}$$

And using the Barenblatt (1962) cohesive relation to specify the stress intensity factor gives in the simplest configuration

$$K = (\mu \sigma_c w_b)^{1/2} \tag{60}$$

Associating r with $\sqrt{A}$, (59) and (60) correspond to (58).

From (54) the velocity of the moving blocks in the breakaway region is

$$u_o = \frac{F_o}{2 (m k_c)^{1/2}} \frac{u_b}{c} = \frac{F_o}{2 (m k_c)^{1/2}} \left(1 - \frac{8 k_c w_b g_o}{F_o^2} \right)^{1/2} \tag{61}$$

And this reduces to (47) in the limit of zero cohesion.

Again, it is of interest to consider the energy balance. The input energy from the potential energy of the downstream springs that enter the breakaway zone is

$$P_i = \frac{1}{2} \frac{F_o^2}{k_c} \frac{u_b}{\delta} = \frac{1}{2} \frac{F_o^2}{(k_c m)^{1/2}} \left(1 - \frac{8 k_c w_b g_o}{F_o^2} \right)^{1/2} \tag{62}$$

The kinetic energy imparted to the blocks in the breakaway wave per unit time is

$$P_{KE} = \frac{1}{2} m u_0^2 \frac{u_b}{\delta} = \frac{1}{4} \frac{F_o^2}{(k_c m)^{1/2}} \left(1 - \frac{8 k_c w_b g_o}{F_o^2}\right)^{3/2} \quad (63)$$

And the potential energy imparted to the springs in the breakaway region per unit time is

$$P_{KE} = \frac{1}{\delta} \frac{F_0^2}{k_c} 2 \frac{u_b}{\delta} = \frac{1}{4} \frac{F_o^2}{(k_c m)^{1/2}} \left(1 - \frac{8 k_c w_b g_o}{F_o^2}\right)^{1/2} \quad (64)$$

And the energy required per unit time to break cohesion is

$$P_c = g_o w_b 2 \frac{Ub}{\delta} = 2 g_o w_b \left(\frac{k_c}{m}\right)^{1/2} \left(1 - \frac{8 k_c w_b g_o}{F_0^2}\right)^{1/2} \quad (65)$$

Once again the overall energy balance given in (37) is satisfied as well as the energy division given by (38).

5 The role of driver springs

The solutions given in the two previous sections did not include the driver springs that were included in the derivation of the original model equation (8). We now include the driver springs but must also make further modifications to our basic model. With the driver springs our governing equation (8) becomes the telegraph equation rather than the wave equation. The telegraph equation yields periodic solutions only for supersonic $u_p > c$ waves, these waves have been discussed by Langer and Tang (1991). For a propagating wave, as considered here, supersonic solutions are not acceptable.

In order to obtain acceptable propagating solutions we will include a linear viscous resistance on the rupture surface. Thus we will assume

$$F = g_o \qquad \text{for } 0 < w < w_b \quad (66)$$

$$F = \eta \frac{\partial w}{\partial t} \qquad \text{for } w > w_b \quad (67)$$

Substitution of (66) and (67) into (8) and transforming into a wave fixed coordinate system using (22) gives

$$m \left(c^2 - u_b^2\right) \frac{d^2 w}{d\xi^2} + k_p (w_p - w) = g_o \qquad \text{for } \xi > 0 \quad (68)$$

$$m \left(c^2 - u_b^2\right) \frac{d^2 w}{d\xi^2} + u_b \eta \frac{dw}{d\xi} + k_p (w_p - w) = 0, \qquad \text{for } \xi > 0 \quad (69)$$

As in the previous sections, upstream $\xi > 0$ and downstream $\xi < 0$ solutions will be obtained and they will be matched at the breakaway point $\xi = 0$.

In the upstream region $\xi > 0$ we have the solution

$$w = w_p - \frac{g_o}{k_p} + C_1 e^{\alpha\xi} + C_2 e^{-\alpha\xi} \quad (70)$$

with

$$\alpha^2 = \frac{k_p}{m \left(c^2 - u_b^2\right)} \quad (71)$$

We again satisfy the boundary conditions $w = dw/d\zeta = 0$ at $\xi = \zeta_0$ and $w = w_b$ at $\xi = 0$ and obtain

$$w = \left(\frac{g_o}{k_p} - w_p\right) \left(\cosh\left[\alpha \left(\xi - \xi_o\right)\right] - 1\right) \quad (72)$$

$$w_b = \left(\frac{g_o}{k_p} - w_p\right) \left(\cosh\left(\alpha\xi_o\right) - 1\right) \quad (73)$$

This solution must be matched to the downstream solution.

In the downstream regon $\xi < 0$, the solution of (69) that is finite as $\xi \to -\infty$ and satisfies the condition $w = w_b$ at $\xi = 0$ is

$$w = w_p - (w_p - w_b) e^{\lambda\xi} \quad (74)$$

with

$$m \left(c^2 - u_b^2\right) \lambda + u_b \eta \lambda - k_p = 0 \quad (75)$$

The requirement that $dw/d\xi$ be continuous at $\xi = 0$ requires:

$$\lambda (w_p - w_b) = \left(\frac{g_o}{k_p} - w_p\right) \alpha \sinh\left(\alpha \xi_o\right) \quad (76)$$

From (73) we obtain

$$\sinh\left(\alpha\xi_o\right) = \left(\frac{w_b^2 k_p^2}{\left(g_o - w_p k_p\right)^2} + \frac{2 w_b k_p}{\left(g_o - w_p k_p\right)}\right)^{1/2} \quad (77)$$

It is convenient to introduce nondimensional parameters: The ratio of propagation speed to sound speed

$$M = \frac{u_b}{c} \quad (78)$$

the ratio of the available potential energy to the cohesive energy

$$E = \frac{k_p (w_p - w_b)^2}{2 w_b \left(g_o - k_p w_p + k_p w_b/2\right)} \quad (79)$$

and a viscosity parameter

$$R = \frac{\eta^2}{m k_p} \quad (80)$$

Substitution of (77) and (79) into (76) gives

$$\lambda = \frac{\alpha}{E^{1/2}} \quad (81)$$

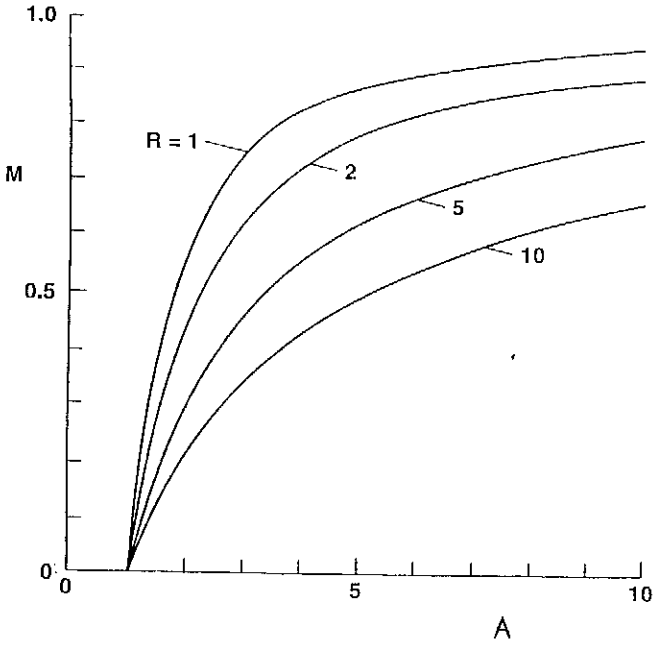

Fig. 5. The ratio of the propagation speed to the sound speed M is given as a function of the energy parameter A for several values of the friction parameter R.

Using (81) to eliminate λ^2 in (75) we obtain

$$\lambda = \frac{k_p (E - 1)}{u_b \eta E} = \frac{\alpha}{E^{1/2}} \tag{82}$$

Since λ must be positive we require $E > 1$ for propagation. Substitution of (71), (78), and (80) into (82) gives

$$M = \left[\frac{1}{1 + \dfrac{ER}{(E - 1)^2}}\right]^{1/2} \tag{83}$$

The nondimensional progagation speed M is related to the energy parameter E and the viscosity parameter R. This result was previously obtained by Langer (1992, eq. 2.11) The dependence of M on E for several values of F is given in Fig. 5. It is seen that we require $E > 1$ for propagation to occur. This propagation threshold is independent of the frictional resistance parameter R. If there is no friction, $R = 0$, then propagation takes place at the speed of sound independent of the potential energy parameter E as long as $E > 1$. As the friction parameter R increases the speed of propagation decreases.

The condition $E = 1$ is equivalent to having

$$w_b \left(g_o - k_p w_p + \frac{1}{2} k_p w_b\right) = \frac{1}{2} k_p (w_p - w_b)^2 \tag{84}$$

This is an energy balance between the energy required to overcome the cohesion of a block $w_b(g_o - k_p w_p + k_p w_b/2)$ and the available potential energy in a driver spring $k_p (w_p - w_b)^2/2$. The right side of (84) must be larger than the left side for a wave to propagated.

We will consider the physical implications of this propagation condition. In order to do this it is appropriate to assume $k_p w_p << g_o$ and $w_b << w_p$ so that the condition for propagation is

$$\frac{k_p w_p^2}{w_b g_o} > 1 \tag{85}$$

Taking $F_p = k_p w_p$ this becomes

$$\frac{F_p^2}{k_p w_b g_o} > 1 \tag{86}$$

which is essentially identical to the condition given in (57).

It is appropriate to introduce a shear stress

$$\tau = \frac{F_p}{A^{1/2} \delta} \tag{87}$$

and a shear modulus

$$\mu = \frac{k_p}{\delta} \tag{88}$$

Introducuing these into (80) along with (39) we obtain

$$\tau = \left(\frac{w_b \sigma_c \mu}{\sqrt{A}}\right)^{1/2} \tag{89}$$

This is our form of the stress intensity factor in analogy with (58).

In order to consider the wave structure and block velocity we introduce the following nondimensional variables along with (9), (11), and (87) and have

$$X = \frac{\xi}{c}\left(\frac{k_p}{m}\right)^{1/2} = \frac{\xi}{\sqrt{A}} \tag{90}$$

$$W = \frac{w_p - w}{w_p - w_b} \tag{91}$$

$$U = \left(\frac{m}{k_p}\right)^{1/2} \frac{1}{(w_p - w_b)} \frac{\partial w}{\partial t} = \frac{\sqrt{A}}{c (w_p - w_b)} \frac{\partial w}{\partial t} \tag{92}$$

From (77) the downstream structure of the breakaway wave is given by

$$W = \exp\left\{\left[\left(\frac{1}{1 - M^2} + \frac{RM^2}{4(1 - M^2)^2}\right)^{1/2} - \frac{R^{1/2} M}{2(1 - M^2)}\right] X\right\} \tag{93}$$

with M being determined from (83). The decay is exponential with a 1/e length

$$X_c = \left[\left(\frac{1}{1 - M^2} + \frac{RM^2}{4(1 - M^2)^2}\right)^{1/2} - \frac{R^{1/2} M}{2(1 - M^2)}\right]^{1/2} \tag{94}$$

This nondimensional width of the breakaway X_c wave is given in Fig. 6 as a function of A for several values of F. The

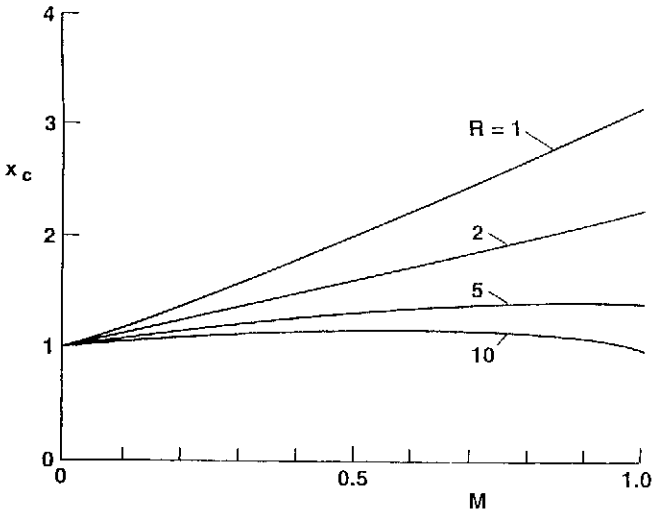

Fig. 6. Dependence of the nondimensional width of the breakaway wave X_c on the ratio of the propagation speed to the sound speed M for several values of the friction parameter R.

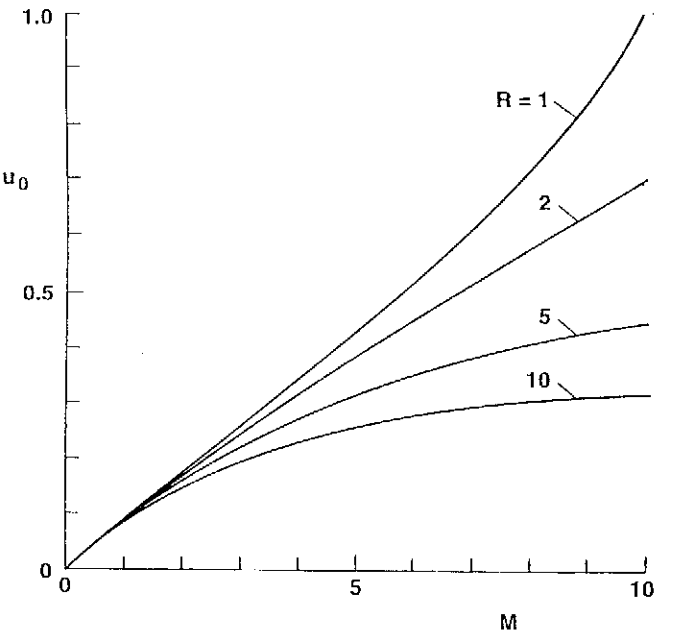

Fig. 7. Dependence of the maximum nondimensional slip velocity U_0 on the ratio of the propagation speed to the sound speed M for several values of the friction parameter R.

nondimensional maximum block velocity at $\xi = 0$, U_0, is given by

$$U_0 = M\left[\left(\frac{1}{1-M^2}+\frac{RM^2}{4(1-M^2)^2}\right)^{1/2}\ \frac{R^{1/2}M}{2(1-M^2)}\right] \qquad (95)$$

The nondimensional maximum slip velocity is given in Fig. 7 as a function of A for several values of R.

We once again consider a specific example. With σ = 10 Mpa and μ = 30 Gpa we have the strain $\varepsilon = \sigma/\mu = 3000^{-1}$. The initial spring displacement is then $w_p = e\ A^{1/2} = 0.333$ m, certainly a reasonable value. For the cohesion parameter we have $(g_o/k_p w_p) = (\sigma_c A^{1/2}/\mu\ w_p) = 3$. Thus from (79) we find E = 1.67. Taking M = 0.5 we find from (81) that R = 0.80. The parameter α defined in (71) has the value $\alpha = [A\ (1 - M^2)]^{1/2} = 1/0.87$ km. The decay length in the downstream region λ^{-1} defined in (74) is evaluated using (82) with the result $\lambda^{-1} = E^{1/2}/\alpha = 1.2$km. The slip velocity at $\xi = 0$, v_{s0}, is given by $v_{vs} = u_b\ w_p\ \lambda = 0.45$ m/s. Again a typical value of the slip velocity on a fault. The viscous stress at $\xi = 0$, $\sigma_{so} = R^{1/2}\ \mu\ v_{vs}/c = 4$ Mpa. This is essentially the stress associated with dynamic friction and compares with the stress σ = 10 Mpa before rupture. The general behavior of this model appears to be a good representation of the behavior of an actual fault.

6 Conclusions

In this paper the problem of dynamic rupture propagation on a fault has been studied using a simple one-dimensional slider-block approximation. The advantage of this approach is that the basic principals of friction are separated from the complexities of a stress concentration at a crack tip. In our models of rupture propagation we consider steady-state rupture propagation and focus our attention on two aspects, surface cohesion and surface resistence. These in turn are related to the concepts of static and dynamic friction.

We directly associate static friction with surface cohesion. If surface displacements are less than a critical value w_b then there is a cohesion force g_0 between the granular materials that constitute a fault. The fault is locked and no displacement takes place. We argue that laboratory measurements carried out at vey low sliding velocities are a measure of these cohesion factors. Locally cohesion is broken but continuous reheals as the constant velocity boundary condition is applied. We furhter argue that these experiments are not relevant to actual faults. The rupture front breaks the cohsive forces in a breakaway zone where the displacemnts and velocities are small.

We associate dynamic friction with a velocity dependent force. If this force decreases with increasing velocity the rupture velocity will approach the sound speed. Since it is known that fault ruptures take place at a fraction, ≈ 0.5, of the sound speed we argue that the dynamic friction force increases with increasing velocity. In this paper we have considered a linear dependence of the shear stress on the slip velocity. The mechanism responsible for the dynamic friction is not yet established. It could be acoustic fluidization of the fault gauge as proposed by Melash (1979, 1995). Or it could be interface waves as proposed by Brune et al. (1993) and by Anooshelpoor and Brune (1994).

References

Anooshelpoor, A., and Brune, J.N., Frictional heat generation and seismic radiation in a foam rubber model of earthquakes, *Pageoph. 142*, 735-747, 1994.

Barenblatt, G.I., The mathematical theory of equilibrium cracks in brittle fracture, *Adv. Ap. Mech., 7*, 55-129, 1962.

Beeler, N.M., Tullis, T.E., and Weeks, J.D., The roles of time and displacement in the evolution effect in rock friction, *Geophys. Res. Let., 21*, 1987-1990, 1994.

Blanpied, M.L., Lockner, D.A., and Byerlee, J.D., An earthquake mechanism based on rapid sealing of faults, *Nature, 358,* 574-576, 1992.

Blanpied, M.L., and Tullis, T.E., the stability of a frictional system with a two state variable constitutive law, *Pageoph, 124,* 413-333, 1986.

Brown, S.R., Scholz, C.H., and Rundle, J.B., A simplified spring-block model of earthquakes, *Geophys. Res. Let., 18,* 215-218, 1991.

Brune, J.N., Brown, S., and Johnson, P.A., Rupture mechanism and interface separation in foam rubber models of earthquakes: a possible solution to the heat flow paradox and the paradox of large overthrusts, *Tectonophys., 218,* 59-67, 1993.

Burridge, R., and Knopoff, L., Model and theoretical seismicity, *Seis. Soc. Am. Bull., 57,* 341-371, 1967.

Byerlee, J., Friction, overpressure and fault normal compression, *Geophys. Res. Let., 17,* 2109-2112, 1990.

Campbell, C.S., Rapid granular flows, *An. Rev. Fluid. Mech., 22,* 57-92, 1990.

Carlson, J.M., Time intervals between characteristic earthquakes and correlations with smaller events: An analysis based on a mechanical model of a fault, *J. Geophys. Res., 96,* 4255-4267, 1991a.

Carlson, J.M., Two-dimensional model of a fault, *Phys. Rev., A44,* 6226-6232, 1991b.

Carlson, J.M., Grannan, E.R., Singh, C. and Swindel, G.H., Fluctuations in self-organizing systems, *Phys. Rev., E48,* 688-698, 1993a.

Carlson, J.M., Grannan, E.R., and Swindel, G.H., Self-organizing systems at finite driving rates, *Phys. Rev., E47,* 93-105, 1993b.

Carlson, J.M., and Langer, J. S., Mechanical model of earthquakes generated by fault dynamics, *Phys. Rev., A40,* 6470-6484, 1989.

Carlson, J.M., Langer, J.S., Shaw, B.E., and Tang, C., Intrinsic properties of a Burridge-Knopoff model of an earthquake fault, *Phys. Rev., A44,* 884-897, 1991.

Christensen, K., and Olami, Z., Variation of the Gutenberg-Richter b values and nontrivial temporal correlations in a spring-block model for earthquakes, *J. Geophys. Res., 97,* 8729-8735, 1992.

Comninou, M., and Dundurs, J., Elastic interface waves involving separation, *J. Ap. Mech, 44,* 222-226, 1977.

Comninou, M., and Dundurs, J., Elastic interface waves and sliding between two solids, *J. Ap. Mech., 45,* 325-330, 1978.

de Sousa Vieira, M., Self-organized criticality in a deterministic mechanical model, *Phys. Rev., A46,* 6288-6293, 1992.

de Sousa Vieira, M., and Herrmann, H.J., Self-similarity of friction laws, *Phys. Rev., E49,* 4534-4541, 1994.

de Sousa Vieira, M., Vasconcelos, G.L., and Nagel, S.R., Dynamics of spring-block models: Tuning to criticality, *Phys. Rev., E47,* R2221-R2224, 1993.

Dieterich, J.H., Time-dependent friction in rocks, *J. Geophys. Res., 77,* 3690-3697, 1972.

Dieterich, J.H., Time-dependent friction and the mechanics of stick-slip, *Pageoph., 116,* 790-806, 1978.

Dieterich, J.H., Modeling of rock friction, 1. Experimental results and constitutive equations, *J. Geophys. Res., 84,* 2161-2168, 1979.

Dieterich, J.H., and Conrad, G., Effect of humidity on time and velocity-dependent friction of rocks, *J. Geophys. Res., 89,* 4196-4202, 1984.

Feder, H.J.S., and Feder, J., Self-organized criticality in a stick-slip process, *Phys. Rev. Let., 66,* 2669-2672, 1991.

Freund, L.B., Comment on "Elastic interface waves involving separation", *J. Ap. Mech., 45,* 226-227, 1978.

Heaton, T.H., Evidence for and implications of self-healing pulses of slip in earthquake rupture, *Phys. Earth Planet. Int., 64,* 1-20. 1990.

Huang, J., and Turcotte, D.L., Are earthquakes an example of deterministic chaos? *Geophys. Res. Let., 17,* 223-226, 1990.

Huang, J., and Turcotte, D.L., Chaotic seismic faulting with a mass-spring model and velocity-weakening friction, *Pageoph., 138,* 569-589, 1992.

Huang, J., Narkounskaia, G., and Turcotte, D.L., A cellular automation, slider-block model for earthquakes 2. Demonstration of self-organized criticality for a two dimensional system, *Geophys. J. Int., 111,* 259-269, 1992.

Ito, K.M. and Matsuzaki, M., Earthquakes as self-organized critical phenomena, *J. Geophys. Res., 95,* 6853-6860, 1990.

Johnston, M.J.S., Linde, A.T., Gladwin, M.T., and Borcherdt, R.D., Fault failure with moderate earthquakes, *Tectonophys., 144,* 198-206, 1987.

Knopoff, L., Landoni, J.A. and Abinante, M. S., Dynamical model of an earthquake fault with localization, *Phys. Rev., A46,* 7445-7449, 1993.

Kosloff, D.D., and Liu, H.P., Reformulation and discussion of mechanical behavior of the velocity dependent friction law proposed by Dieterich, *Geophys. Res. Let., 7,* 913-916, 1980.

Langer, J.S., Models of crack propagation, *Phys. Rev., A46,* 3123-3131, 1992.

Langer, J.S., Dynamic model of onset and propagation of fracture, *Phys. Rev. Let., 70,* 3592-3594, 1993.

Langer, J.S., and Nakanishi, H., Models of crack propagation II. Two-dimensional model with dissipation on the fracture surface, *Phys. Rev., E48,* 439-448, 1993.

Langer, J.S., and Tang, C., Ruptue propagation in a model of an earthquake fault, *Phys. Rev. Let., 67,* 1043-1046, 1991.

Linker, M.F., and Dieterich, J.H., Effects of variable normal stress on rock friction: Observations and constitutive equations, *J. Geophys. Res., 97,* 4923-4940, 1992.

Lorenzetti, E., and Tullis, T.E., "Geodetic predictions of a strike-slip fault model: Implications for intermediate and short-term earthquake prediction, *J. Geophys. Res., 94,* 12,343-12,361, 1989.

Matsuzaki, M., and Takayasu, H., Fractal features of the earthquake phenomenon and a simple mechanical model, *J. Geophys. Res., 96,* 19,925-19,931, 1991.

Melosh, H.J., Acoustic fluidization: A new geologic process?, *J. Geophys. Res., 84,* 7513-7520, 1979.

Melosh, H.J., Dynamical weakening of faults by acoustic fluidization, *Nature,* 379, 601-606, 1996.

Mora, P., and Place, D., Simulation of the frictional stick-slip instability, *Pure Ap. Geophys., 143,* 61-87, 1994.

Morgan, J.D., Turcotte, D.L., and Ockendon, J.R., Models for earthquake rupture propagation, *Tectonophys., 277,* 209-217, 1997.

Myers, C.R., and Langer, J.S., Rupture propagation, dynamical front selection, and the role of small length scales in a model of an earthquake fault, *Phys. Rev., E47,* 3048-3056, 1993.

Nakanishi, H., Cellular automation model of earthquakes with deterministic dynamics, *Phys., Rev., A41,* 7086-7089, 1990.

Nakanishi, H., Statistical properties of the cellular automata model for earthquakes, *Phys. Rev., A43,* 6613-6621, 1991.

Nakanishi, H., Continuum model of mode-III crack propagation with surface friction, *Phys. Rev., E49,* 5412-5419, 1994.

Narkounskaia, G., and Turcotte, D.L., A cellular-automata, slider-block model for earthquakes 1. Demonstration of chaotic behavior for a low order system, *Geophys. J. Int., 111,* 250-258, 1992.

Okubo, P.G., Dynamic rupture modeling with laboratory-derived constitutive relations, *J. Geophys. Res., 94,* 12,321-12,335, 1989.

Okubo, P.G., and Dieterich, J.H., State variable fault constitutive relations for dynamic slip, *Am. Geopys. Un. Mono., 37,* 25-35, 1986.

Pepke, S.L., and Carlson, J.M., Predictability of self-organizing systems, *Phys. Rev., E50,* 236-242, 1994.

Pepke, S.L., and Carlson, J.R. and Shaw, B.E., Prediction of large events on a dynamical model of a fault, *J. Geophys. Res., 99,* 6769-6788, 1994.

Pollock, H.M., Surface forces and adhesion, in *Fundamentals of Friction: Macroscopic and Microscopic Processes,* I.L. Singer and H.M. Pollock, eds., pp. 77-94, Kluwer, Dordrecht, 1992.

Rice, J.R., Spatio-temporal complexity of slip on a fault, *J. Geophys. Res., 98,* 9885-9907, 1993.

Ruina, A., Slip instability and state variable friction laws, *J. Geophys. Res., 88,* 10,359-10,370. 1983.

Rundle, J.B., and Brown, S.R., Origin of rate dependence in frictional sliding, *J. Stat. Phys., 65,* 43-412, 1991.

Rundle, J.B. and Klein, W., Scaling and critial phenomena in a cellular automaton slider-block model for earthquakes, *J. Stat. Phys., 72,* 405-412, 1993.

Savage, S.B., The mechanics of rapid granular flows, *Adv. Ap. Mech., 24,* 289-366, 1984.

Schallamach, A., How does rubber slide, *Wear, 17,* 301-312, 1971.

Scholz, C.H., *The Mechanics of Earthquakes and Faulting,* Cambridge University Press, Cambridge, 1990.

Shaw, B.E., Carlson, J.M., amd Langer, J.S., Patterns of seismic activity preceeding large earthquakes, *J. Geophys. Res., 97,* 479-488, 1992.

Sleep, N.H., and Blanpied, M.L., Creep, compaction and the weak rheology of major faults, *Nature, 359,* 687-692, 1992.

Sleep, N.H., and Blanpied, M.L., Ductile creep and compaction: A mechanism for transiently increasing fluid pressure in mostly sealed fault zones, *Pure Ap. Geophys., 143,* 9-40, 1994.

Sornette, A., and Sornette, D., Self-organized criticality and earthquakes, *Europhys. Let., 9,* 197-202, 1989.

Sornette, A., and Sornette, D., Earthquake rupture as a critical point: Consequence for telluric precursors, *Tectonophys., 179,* 327-334, 1990.

Takayasu, H., and Matsuzaki, M., Dynamical transition in threshold elements, *Phys. Let., A131,* 224-247, 1988.

Tolstoi, D.M., Significance of the normal degree of freedom and natural normal vibrations in contact friction, *Wear, 10,* 199-213, 1967.

Tse, S.T., and Rice, J.R., Crustal earthquake instability in relation to the depth variation of frictional slip properties, *J. Geophys. Res., 91,* 9452-9472, 1986.

Vasconcelos, G.L., de Sousa Vieira, M., and Nagel, S.R., Phase transitions in spring-block model of earthquakes, *Physica, A191,* 69-74, 1992.

Weeks, J.D., Constitutive laws for high-velocity frictional sliding and their influence on stress drop during unstable slip, *J. Geophys. Res., 98,* 17,636-17,648, 1993.